Equation of state of nuclear matter from empirical constraints

N. Alam, B. K. Agrawal, J. N. De, and S. K. Samaddar

Saha Institute of Nuclear Physics, 1/AF Bidhannagar, Kolkata 700064, India

G. Colò

Dipartimento di Fisica, Università degli Studi di Milano, via Celoria 16, I-20133 Milano, Italy and INFN, sezione di Milano, via Celoria 16, I-20133 Milano, Italy

From empirically determined values of some of the characteristic constants associated with homogeneous nuclear matter at saturation and subsaturation densities, within the framework of a Skyrme-inspired energy density functional, we construct an equation of state (EoS) of nuclear matter. This EoS is then used to predict values of density slope parameters of symmetry energy $L(\rho)$, isoscalar incompressibility $K(\rho)$, and a few related quantities. The close consonance of our predicted values with the currently available ones for the density dependence of symmetry energy and incompressibility gleaned from diverse approaches offers the possibility that our method may help in settling their values in tighter bounds. Extrapolation of our EoS at supranormal densities shows that it is in good harmony with the one extracted from experimental data.

I. INTRODUCTION

The nuclear equation of state (EoS) entails in a broad sweep knowledge of the diverse properties of nuclear matter: its saturation density, energy per nucleon $e(\rho)$ (ρ is the density), incompressibility $K(\rho)$, the symmetry energy and its density content, i.e., the symmetry coefficient $e_{\rm sym}(\rho)$, the symmetry slope parameter $L(\rho)$, the symmetry incompressibility $K_\tau(\rho)$, and all the higher symmetry derivatives. Attention has been naturally drawn in recent times toward having a refined understanding of this nuclear EoS from both experimental and theoretical sides. The binding energies of stable atomic nuclei are the most accurately known experimental entities in nuclear physics; these supplemented with knowledge of giant monopole and dipole resonances followed by theoretical analysis have yielded some of the EoS parameters such as the saturation density ρ_0 of symmetric nuclear matter and $e(\rho_0)$, $K(\rho_0)$, and $e_{\rm sym}(\rho_0)$ in reasonably tight bounds [1–6]. The knowledge of the symmetry derivatives $L(\rho_0)$ and $K_\tau(\rho_0)$ is still not very certain [1,7–9]. Analyses of the different nuclear observables do not help much in removing the uncertainty. Correlation systematics of nuclear isospin with neutron skin thickness [10,11], isospin diffusion [12,13], nucleon emission ratios [14], or isoscaling [15] in heavy ion collisions, all yield values of the symmetry slope parameter L_0 [$=L(\rho_0)$] that are not much in consonance with one another. An attempt was recently made to constrain L_0 in tighter bounds from nuclear masses aided by microscopic calculations [16,17] on the neutron skin of heavy nuclei; it was found to give $L_0 = 59 \pm 13.0$ MeV. Other recent attempts, from analysis of the isovector giant dipole and quadrupole resonances in the ^{208}Pb nucleus [18,19] give $L_0 = 43 \pm 26$ and 37 ± 18 MeV respectively. This underscores the still unresolved uncertainty in getting to the value of L_0 and asks for newer avenues to understand it. The present state of the art on symmetry energy and related parameters can be found in the topical issue on nuclear symmetry energy [20].

The EoS parameters so mentioned pertain to only one density: the saturation density ρ_0. If all of them are known precisely, it is in principle possible to construct with a suitable energy density functional (EDF) the nuclear EoS $e(\rho,\delta)$ where $\delta = (\rho_n - \rho_p)/(\rho_n + \rho_p)$ is the isospin asymmetry. Whereas the high density end of the EoS would be of immediate value in understanding the dynamical evolution of the core collapse of a massive star and the associated explosive nucleosynthesis [21,22], or the radii and lower bound of the maximum mass of cold neutron stars [23], the low-density end helps in getting a closer estimate of the neutron skin thickness or the neutron density distribution [10,11,16,17] in neutron-rich nuclei. Accurate knowledge about the EoS parameters at densities other than ρ_0 may put the nuclear EoS on firmer ground; unfortunately, they are very scanty. At density higher than ρ_0, information from experimental data has still large uncertainty [24]; at subsaturation density, from giant dipole resonance analysis, a quantitative constraint on $e_{\rm sym}(\rho)$ could be put as $23.3 < e_{\rm sym}(\rho = 0.1 \text{ fm}^{-3}) < 24.9$ MeV [7]. Further information derived from theoretical analyses at around this density may be of added significance: (i) the energy per nucleon of neutron matter is $\sim 10.9 \pm 0.5$ MeV at $\rho = 0.1$ fm^{-3} [25] and (ii) the density derivative of the nuclear incompressibility $M_c = 3\rho \, dK/d\rho|_{\rho=\rho_c} \simeq 1100 \pm 70$ MeV where ρ_c is $\simeq 0.7\rho_0$ [26].

As is evident from the previous discussion, the plethora of nuclear EoS failed to effectively constrain the density content of the nuclear symmetry energy and the nuclear incompressibility from fits to diverse microscopic nuclear data. The reason lies in the choice of different sets of microscopic observables to be fitted. The isoscalar and isovector quantities associated with nuclear matter, however, have emerged to be very well constrained. The isoscalar entities are (i) e_0 [$=e(\rho_0) = -16.0 \pm 0.1$ MeV], (ii) saturation density ρ_0 (=0.155 ± 0.008 fm^{-3}), where the pressure $P(\rho_0) = 0$, and (iii) the incompressibility coefficient K_0 [$=K(\rho_0) = 9\partial^2 e/\partial \rho^2|_{\rho_0} = 9 dP/d\rho|_{\rho_0} = 240 \pm 20$ MeV] [27]. All these

quantities refer to symmetric nuclear matter. The isovector quantities are (iv) $e_{\text{sym}}(\rho_0)$ (=32.1 ± 0.31 MeV) [4] and (v) $e_{\text{sym}}(\rho = 0.1\text{fm}^{-3})$ (=24.1 ± 0.8 MeV) [7].

In this article, we have tried to find how the input of the empirical knowledge of these quantities can be used to construct an EDF for nuclear matter and to predict the as yet not so well-constrained density dependence of its symmetry properties in reasonably tighter bounds. These isoscalar and isovector nuclear parameters effectively contain condensed experimental information on the bulk nuclear properties. As opposed to direct investigation of the microscopic properties of nuclei as done, e.g., in Ref. [28], which can lead to somewhat different predictions depending on the observables chosen to be explored, the alternate edifice for the nuclear EDF built in this article on the well established nuclear bulk parameters is so structured, as we see later, that it gives an easy and transparent look at the correlations of the predicted values of the density derivatives of the symmetry energy and the nuclear incompressibility to the input parameters. Furthermore, if the values of the density derivatives L_0, K_τ, M_0, etc. could be well settled by as yet other unexplored means and differ from our predicted values, the foundation, i.e., the values of the nuclear bulk parameters or the choice of the Skyrme EDF, then become subjects of fresher scrutiny. Computationally, our method is also much less intensive. To our knowledge, a comprehensive study of this kind has not been done before.

Henceforth, the quantities corresponding to the densities ρ_0 and $\rho = 0.1$ fm^{-3} will be denoted with the subscripts 0 and 1, respectively (like $e_{\text{sym},0}$, $e_{\text{sym},1}$, etc.). The value of ρ_0 is an indirectly obtained entity. From acceptable Skyrme energy density functionals, it is ~ 0.16 fm^{-3} [29] whereas the relativistic mean-field models give a value of ρ_0 in the vicinity of ~ 0.15 fm^{-3} [30,31]. Our choice for ρ_0 covers this range.

The paper is organized as follows. Section II contains a brief discussion of the theoretical elements. Results and discussions are presented in Sec. III. Section IV contains the concluding remarks.

II. THEORETICAL EDIFICE

The Skyrme framework is chosen for the energy density functional [32]. The energy per nucleon for nuclear matter is then

$$
\begin{aligned}
e(\rho,\delta) = {} & a_1 \left[\left(\frac{1+\delta}{2} \right)^{5/3} + \left(\frac{1-\delta}{2} \right)^{5/3} \right] \rho^{2/3} \\
& + (b_1 + b_2 \delta^2)\rho + (c_1 + c_2 \delta^2)\rho^{\alpha+1} \\
& + \left[d_1 \left\{ \left(\frac{1+\delta}{2} \right)^{5/3} + \left(\frac{1-\delta}{2} \right)^{5/3} \right\} \right. \\
& \left. + d_2 \left\{ \left(\frac{1+\delta}{2} \right)^{8/3} + \left(\frac{1-\delta}{2} \right)^{8/3} \right\} \right] \rho^{5/3}. \quad (1)
\end{aligned}
$$

The first term on the right-hand side is the free Fermi gas energy, $a_1 = \frac{\hbar^2}{2m} \frac{3}{5}(3\pi^2)^{2/3} = 119.14$ MeV fm^2, where m is the nucleon mass. For the chosen values of e_0 and ρ_0, values of α ranging only from 1/6 to 1/3 allow for an acceptable set of

$(m^*/m, K_0)$ [33] where m^* is the nucleon effective mass. We therefore chose $\alpha = 0.2 \pm 0.1$; this allows m^*/m to lie in the acceptable range $m^*/m \simeq 0.8 \pm 0.2$ [29]. We take the median value of $\alpha = 0.2$. We are left with six unknown parameters, namely, b_1, c_1, d_1, b_2, c_2, and d_2, which would completely define the EDF. As already mentioned, we have, however, five equations, three from isoscalar entities and two from isovector entities.

The isoscalar equations are

$$
e_0 = \frac{a_1}{2^{2/3}} \rho_0^{2/3} + b_1 \rho_0 + c_1 \rho_0^{\alpha+1} + \left(\frac{1}{2^{2/3}}d_1 + \frac{1}{2^{5/3}}d_2 \right) \rho_0^{5/3}, \quad (2)
$$

$$
\begin{aligned}
P_0 = 0 = {} & \rho_0^2 \left[\frac{2}{3} \frac{a_1}{2^{2/3}} \rho_0^{-1/3} + b_1 + c_1(\alpha+1)\rho_0^\alpha \right. \\
& \left. + \frac{5}{3} \left(\frac{1}{2^{2/3}}d_1 + \frac{1}{2^{5/3}}d_2 \right) \rho_0^{2/3} \right], \quad (3)
\end{aligned}
$$

and

$$
\begin{aligned}
K_0 = 9 \left[\frac{10}{9} \frac{a_1}{2^{2/3}} \rho_0^{2/3} + 2b_1\rho_0 + (\alpha+1)(\alpha+2)c_1\rho_0^{\alpha+1} \right. \\
\left. + \frac{40}{9} \left(\frac{1}{2^{2/3}}d_1 + \frac{1}{2^{5/3}}d_2 \right) \rho_0^{5/3} \right]. \quad (4)
\end{aligned}
$$

The isoscalar equations yield the values of b_1, c_1, and $(\frac{d_1}{2^{2/3}} + \frac{d_2}{2^{5/3}})$. The isovector equations, evaluated at ρ_0 and ρ_1 (=0.1 fm^{-3}) are given by

$$
\begin{aligned}
e_{\text{sym}}(\rho) &= \frac{1}{2} \frac{\partial^2 e(\rho)}{\partial \delta^2} \bigg|_{\delta=0} \\
&= \frac{5}{9} \frac{a_1}{2^{2/3}} \rho^{2/3} + b_2\rho + c_2\rho^{\alpha+1} \\
&\quad + \left[\frac{5}{9} \frac{d_1}{2^{2/3}} + \frac{20}{9} \frac{d_2}{2^{5/3}} \right] \rho^{5/3}. \quad (5)
\end{aligned}
$$

To fix the remaining parameters, we need an extra condition in conjunction with the two isovector equations. For this, we take that the energy per particle of isospin asymmetric nuclear matter is quadratic in the asymmetry parameter δ. This condition is found to be an excellent approximation from nearly all energy density functionals [34,35] and also from microscopic calculations in the Bruckner-Hartree-Fock (BHF) formalism [36,37] at all densities up to ρ_0 and a little beyond. This implies that the difference between the symmetry energy coefficients defined by Eq. (5) and the one by the equation

$$
\begin{aligned}
\tilde{e}_{\text{sym}}(\rho) &= e(\rho,\delta=1) - e(\rho,\delta=0) \\
&= a_1 \left(1 - \frac{1}{2^{2/3}} \right) \rho^{2/3} + b_2\rho + c_2\rho^{\alpha+1} \\
&\quad + \left[d_1 \left(1 - \frac{1}{2^{2/3}} \right) + d_2 \left(1 - \frac{1}{2^{5/3}} \right) \right] \rho^{5/3}, \quad (6)
\end{aligned}
$$

should be minimal.

To achieve this minimality, we take the help of the equation for the symmetry slope parameter L. From its definition
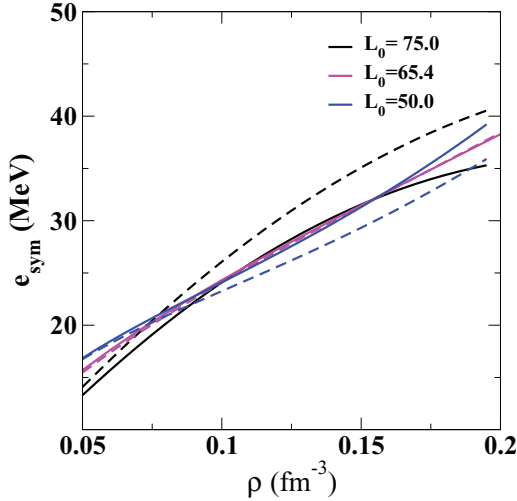
FIG. 1. (Color online) Plots for the variation of e_{sym} as a function of density ρ. The values of e_{sym} represented by the full and the dashed lines are obtained using two different definitions as given by Eqs. (5) and (6). The blue, magenta, and black lines correspond to $L_0 = 50$, 65.4, and 75 MeV at $\rho = \rho_0$. With $L_0 = 65.4$ MeV, one magenta line falls over the other; they can-not be distinguished from each other.

$L(\rho) = 3\rho \partial e_{\text{sym}}/\partial \rho$, one gets from Eq. (5)

$$L(\rho) = 3\rho \left[\frac{10}{27} \frac{a_1}{2^{2/3}} \rho^{-1/3} + b_2 + (\alpha+1)c_2\rho^{\alpha} \right.$$
$$\left. + \frac{5}{3}\rho^{2/3} \left(\frac{5}{9}\frac{d_1}{2^{2/3}} + \frac{20}{9}\frac{d_2}{2^{5/3}} \right) \right], \quad (7)$$

With a given value of L_0 $[=L(\rho_0)]$, from known $e_{\text{sym},0}$ and $e_{\text{sym},1}$, at the two densities ρ_0 and ρ_1, one can solve for b_2, c_2, and $[\frac{5}{9}\frac{d_1}{2^{2/3}} + \frac{20}{9}\frac{d_2}{2^{5/3}}]$. Since $(\frac{d_1}{2^{2/3}} + \frac{d_2}{2^{5/3}})$ is known from the isoscalar equations, d_1 and d_2 are now obtained.

Now that for a given L_0 all the parameters of the EDF are known, one can calculate $e_{\text{sym}}(\rho)$. With the same set of coefficients $\tilde{e}_{\text{sym}}(\rho)$ can also be calculated. Normally, for an arbitrary value of the given L_0, e_{sym} and $\tilde{e}_{\text{sym}}$ may not be equal; only for a specific value of L_0 do they tend to be equal (see Fig. 1). To be more specific, as a function of input L_0, we have calculated the coefficients b_1, b_2, etc. using the relevant equation for e_{sym} for a set of densities ρ_i lying in the range $0.05 < \rho < 0.2$ fm^{-3}, calculated $\tilde{e}_{\text{sym}}$ with the same set of coefficients, and have chosen that L_0 as the requisite one that gives the minimum of $\sum_i [e_{\text{sym}}(\rho_i) - \tilde{e}_{\text{sym}}(\rho_i)]^2$. This settles the EoS. In Fig. 1, $e_{\text{sym}}(\rho)$ and $\tilde{e}_{\text{sym}}(\rho)$ are displayed as a function of input L_0. The full lines refer to $e_{\text{sym}}(\rho)$, the dashed lines to $\tilde{e}_{\text{sym}}(\rho)$. The difference between these two is minimum when $L_0 = 65.4$ MeV. All the parameters a_1, b_1, b_2, etc. corresponding to the density functional are listed in Table I.

III. RESULTS AND DISCUSSIONS

Once the parameters of the EDF [Eq. (1)] are known, the higher order density derivatives of energy and symmetry energy of nuclear matter may be obtained. They are presented

TABLE I. Parameters of the energy density functional corresponding to the central values of the isoscalar and isovector inputs.

a_1 (MeV fm^2)	119.14	α	0.2
b_1 (MeV fm^3)	-816.95	b_2 (MeV fm^3)	744.65
c_1 (MeV fm$^{3(\alpha+1)}$)	724.51	c_2 (MeV fm$^{3(\alpha+1)}$)	-1149.66
d_1 (MeV fm^5)	-32.99	d_2 (MeV fm^5)	891.15

in Sec. III A. This EDF can also be used to estimate certain properties of microscopic nuclei like neutron skin thickness of heavy nuclei. This is discussed in Sec. III B. As an aside, the EDF has also been employed to explore some properties of neutron stars, discussion of which is contained in Sec. III C.

A. Nuclear matter: Density derivatives of symmetry energy and isoscalar incompressibility

Expressions for higher order symmetry derivatives $K_{\text{sym},0}$ and K_τ are given by $K_{\text{sym},0} = 9\rho_0^2 \frac{\partial^2 e_{\text{sym}}}{\partial\rho^2}|_{\rho_0}$ and $K_\tau = 9\rho_\delta^2 \frac{\partial^2 e_{\text{sym}}}{\partial\rho^2}|_{\rho_\delta}$. Here ρ_δ is the saturation density of asymmetric nuclear matter corresponding to the asymmetry δ. The symmetry derivatives $K_{\text{sym},0}$ and K_τ are related: $K_\tau = K_{\text{sym},0} - 6L_0 - \frac{Q_0 L_0}{K_0}$, where $Q_0 = 27\rho_0^3 \frac{\partial^3 e(\rho,0)}{\partial\rho^3}|_{\rho_0}$. They all can be evaluated from the EDF parameters. The density derivative of the isoscalar incompressibility $M(\rho) (= 3\rho \frac{dK(\rho)}{d\rho})$ of symmetric nuclear matter is also calculated. At the saturation density ρ_0, $M_0(=M(\rho_0))$ equals $12K_0 + Q_0$. In Table II we list the calculated values of various isoscalar and isovector quantities together with their total uncertainties. The latter are associated with the uncertainties in the six input quantities Y_i ($=\{e_0, \rho_0, K_0, e_{\text{sym},0}, e_{\text{sym},1}, \text{ and } \alpha\}$). The extracted value of L_0 is 65.4 ± 13.5 MeV. It is in excellent consonance with that obtained from analysis of pygmy dipole resonance [38] and in very good agreement with that obtained earlier from nuclear masses and the neutron skin thickness of heavy nuclei [16,17]. This is also very consistent with the value $L_0 = 66.5$ MeV obtained from a systematic analysis within the BHF approach using a realistic nucleon-nucleon potential [39]. Not much can be said about the reasons behind the good agreement between our present extracted value of L_0 with that obtained from pygmy dipole resonance [8] except that in this case the value of $e_{\text{sym}}(\rho_0)$ matches extremely well with our input value. The agreement with that obtained from the BHF approach [39] is possibly coincidental; the one aspect that is to be noted here is that all the symmetry derivatives L_0, $K_{\text{sym},0}$, and K_τ from the BHF approach are in extremely good consonance with our calculated values though the nuclear bulk parameters [ρ_0, e_0, K_0, and $e_{\text{sym}}(\rho_0)$] do not have a good common overlap.

TABLE II. Values of the extracted entities from the nuclear EoS. All quantities are in MeV.

L_0	65.4 ± 13.5	M_c	1150 ± 91
$K_{\text{sym},0}$	-22.9 ± 73.2	Q_0	-344 ± 56
K_τ	-321.6 ± 34.4	M_0	2535 ± 293

TABLE III. The observables X are listed in the first column, they are in units of MeV. The second column represents ΔX, the total uncertainty in X from the input uncertainties ΔY_i in the vector **Y** $\{e_0, \rho_0, K_0, e_{\text{sym},0}, e_{\text{sym},1}, \alpha\}$. The element $Y_2 (\equiv \rho_0)$ is in unit of fm^{-3}, $Y_6 (\equiv \alpha)$ is dimensionless, all other elements in the vector **Y** are in units of MeV. The units in the columns $\frac{\partial X}{\partial Y_i}$ ($i = 1, .. 6$) can then be obtained accordingly.

X	ΔX	$\frac{\partial X}{\partial Y_1}$	$\frac{\partial X}{\partial Y_2}$	$\frac{\partial X}{\partial Y_3}$	$\frac{\partial X}{\partial Y_4}$	$\frac{\partial X}{\partial Y_5}$	$\frac{\partial X}{\partial Y_6}$
L_0	13.5	0.6	−1118	0.081	10.16	−11.09	−27.5
K_{sym}	73.2	12.2	−3889	1.502	25.84	−40.07	−489
K_τ	34.4	−5.4	1339	0.024	−20.55	10.59	309.2
M_0	293	54	−447.5	14.6	0.00	0.00	−195
M_c	91	−2.9	57.5	4.55	0.00	0.00	32.6
Q_0	56	54	−447.5	2.6	0.00	0.00	−194.9

Most of the uncertainty in our extracted value of L_0 comes from the uncertainties in the empirically obtained quantities ρ_0 and $e_{\text{sym}}(\rho)$ at the two densities (see also Table III). If the central value of ρ_0 is pushed down to 0.14 fm^{-3} keeping all other input parameters same, then the central value of L_0 shoots up to 86.1 MeV. Attention is also drawn to the calculated value of K_τ. Analyzing the experimental breathing-mode energies of Sn isotopes, Li *et al.* [40] suggested its value as -550 ± 100 MeV. This is too strongly negative to be compatible with the behavior of low-density neutron matter [41,42]. Higher order effects such as surface symmetry, present in such analysis in disguise, may have contributed to such a high value. Explicit inclusion of the surface symmetry term seems to lower the value of K_τ to ~ -350 MeV [43,44]. Our present value of $K_\tau = -321.6 \pm 34.4$ MeV is in very good agreement with this; it is also in close consonance with the value of -370 ± 120 MeV extracted from measurements of isospin diffusion in heavy ion collisions. The empirical value of M_c (=1100 ± 70 MeV) obtained from analysis of giant monopole resonance energies of Sn isotopes and of ^{90}Zr and ^{144}Sm nuclei [26] is very compatible with our calculated value; similarly, the value of Q_0 calculated by us conforms well with the one ($Q_0 = -350 \pm 30$ MeV) obtained from examination of a host of standard Skyrme interactions [34].

The total uncertainties in the various quantities considered in Table II are evaluated as [45]

$$\Delta X = \sqrt{\sum_i (\Delta X_i)^2}, \quad (8)$$

where $\Delta X_i = \frac{\partial X}{\partial Y_i} \Delta Y_i$; ΔX is the total uncertainty on a given quantity X induced by the associated uncertainties ΔY_i (= 0.1 MeV, 0.008 fm^{-3}, 20 MeV, 0.31 MeV, 0.8 MeV, 0.1) in the input quantities Y_i. The quantities $\frac{\partial X}{\partial Y_i}$ are calculated numerically; their signs reflect the direction of change in X with increase in Y_i. Table III displays, for the relevant observables X, the values of $\frac{\partial X}{\partial Y_i}$ along with the associated total uncertainty ΔX. The derivatives $\frac{\partial X}{\partial Y_i}$ help in estimating the partial contributions ΔX_i to the total uncertainty ΔX. Once $\frac{\partial X}{\partial Y_i}$ are known, it is easy to estimate the change in ΔX with change in ΔY_i. This table can be an instructive guide in
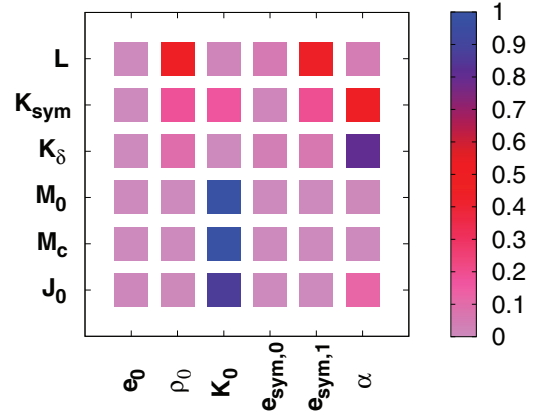

FIG. 2. (Color online) The normalized squared errors, $(\frac{\partial X}{\partial Y_i} \frac{\Delta Y_i}{\Delta X})^2$ ($= x_i^2$), are color coded. The quantities X and Y_i are given along the ordinate and abscissa respectively.

improving existing energy density functionals as it enables one to understand how the various quantities X can be adjusted by changing Y_i's or vice versa. One may note that the symmetry observables L_0, $K_{\text{sym},0}$, and K_τ correlate with $e_{\text{sym},0}$ and $e_{\text{sym},1}$ always in the reverse (see columns 6 and 7 in Table III). This correlated structure of L_0 on $e_{\text{sym},0}$ and $e_{\text{sym},1}$ was noticed earlier [46]. Similar correlation of the symmetry observables $K_{\text{sym},0}$ and K_τ on $e_{\text{sym},0}$ and $e_{\text{sym},1}$ is noticed in our calculation.

The fractional contributions $x_i^2 = (\frac{\Delta X_i}{\Delta X})^2 = (\frac{\partial X}{\partial Y_i} \frac{\Delta Y_i}{\Delta X})^2$ to the uncertainties in the observables X from the uncertainties in the input quantities Y_i are shown in Fig. 2 in color code. As one sees, $\sum_i x_i^2 = 1$. They depict the relative importance of the precision of the input parameters in measuring up the uncertainties in an observable X. From the first column in the figure, on can easily see that the uncertainty in energy per particle e_0 has a negligible role in the uncertainties in the observables X we calculate. One also sees that nearly all the uncertainties in M_0 and M_c emanate from the uncertainty in K_0 and that the uncertainty in α has a very strong role in the evaluated uncertainty of K_τ.

B. Finite nuclei: Neutron skin

The EoS of infinite homogeneous nuclear matter calculated from the EDF can be beneficially used to estimate some quantities relevant to microscopic nuclear systems. For example, with the calculated values of L_0 and $K_{\text{sym},0}$, one can evaluate ρ_A, the equivalent density of nuclei, from the equation

$$e_{\text{sym}}^s \simeq A^{1/3} \left[L_0 \epsilon_A - \frac{1}{2} K_{\text{sym},0} \epsilon_A^2 \right], \quad (9)$$

where, e_{sym}^s is the surface symmetry energy coefficient. The equivalent density ρ_A of a nucleus of mass A is defined as the density at which the symmetry coefficient $e_{\text{sym}}(\rho_A)$ of nuclear matter equals $e_{\text{sym}}(A)$, the symmetry coefficient of the nucleus. The "experimental" value of e_{sym}^s is taken as 58.91 ± 1.08 MeV [4]; $\epsilon_A = (\rho_0 - \rho_A)/3\rho_0$. Figure 3 displays our calculated values of ρ_A (shown as a shaded region) as a function of the atomic mass number A. The blue triangles in the figure refer to the value of ρ_A from Table I of Ref. [10], calculated with different effective interactions for three nuclei,
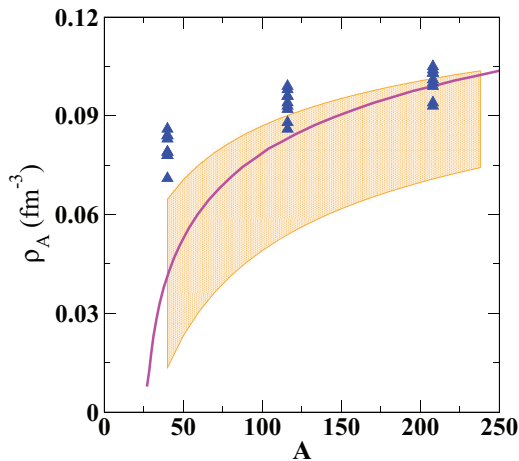
FIG. 3. (Color online) Our results for the equivalent density shown as a shaded region as a function of mass number. The blue triangles are from Ref. [10], the magenta line is from Ref. [6].

$A = 40$, 116, and 208. The magenta line corresponds to the values calculated in Ref. [6]. Our calculations with the indicated errors are seen to have a good overlap with these results. With known L_0, an estimate of r_{skin}, the neutron-skin thickness of heavy nuclei, can also be made. For that we make use of the $L_0 - r_{skin}$ correlation method as elucidated in Refs. [10,17] for Skyrme interactions. As an example, with our value of L_0 we obtain $r_{skin} \simeq 0.21 \pm 0.02$ fm for ^{208}Pb. Some deliberations at this stage on the neutron skin r_{skin} of ^{208}Pb may be meaningful. A recent PREX experiment [47] reports a large central value of 0.33 fm for r_{skin} of ^{208}Pb with very large error bars. This contradicts nearly all the calculated results of r_{skin}, which are comparatively much smaller. Fattoyev and Piekarewicz [48] devised a relativistic EoS that can accommodate such a large neutron skin, but then $e_{sym}(\rho_0)$ and L_0 become uncomfortably high. The larger the value of r_{skin}, the larger becomes the value of L_0. It is known that the larger is then the value of the neutron star radius [49]. A large neutron star radius seems to be incompatible with astrophysical data [50,51]; a very large value for the neutron skin of ^{208}Pb is thus doubtful. Calculations by Brown [25] tend to disfavor a large neutron skin of ^{208}Pb. Nuclear ground state data for closed shell nuclei were fitted with a set of Skyrme interactions with constraints of fixed r_{skin}. The average deviation for binding energies was found to be similar for $r_{skin} = 0.16$ and 0.20 fm, but increased by 0.1 to 0.3 MeV for $r_{skin} = 0.24$ fm. A very recent experimental determination of the neutron skin thickness from coherent pion production [52] adds a new dimension to this issue: the extracted value of r_{skin} for ^{208}Pb is $r_{skin} = 0.15 \pm 0.03$ fm.

C. Supranormal densities: Neutron stars

Having come this far, we try to assess our EoS with reference to that extracted from experimental data at supranormal densities. This is done in Fig. 4. The upper panel displays the EoS (pressure density relation) of symmetric nuclear matter (SNM). The shaded red and yellow regions show the
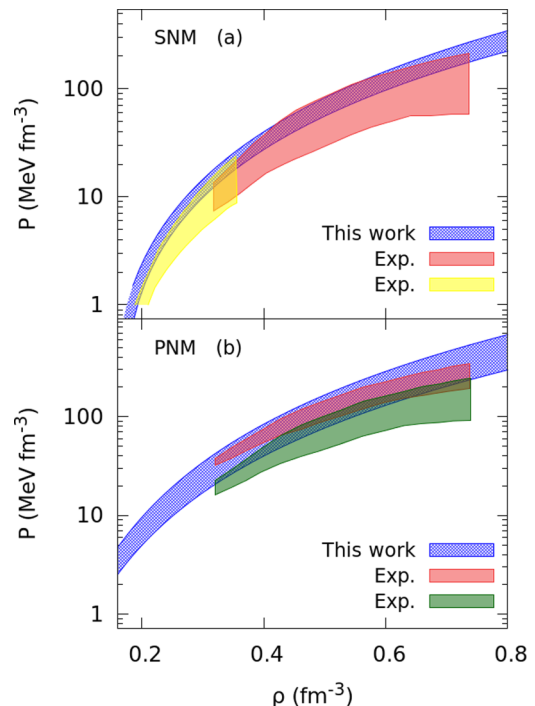

FIG. 4. (Color online) The EoS for symmetric nuclear matter (upper panel) and for pure neutron matter (lower panel). The red, yellow, and green shaded regions represent the experimental data taken from Refs. [53–56]. The blue shaded regions are the EoS obtained in this work. See text for details.

"experimental" EoS for SNM synthesized from collective flow data [53] and from data for kaon production [54,55], respectively; the blue shaded region shows ours. The EoS of pure neutron matter (PNM) has an additional repulsive component coming from the density dependence of symmetry energy. This part of the EoS is laced with uncertainty; it is model dependent. The lower panel shows the EoS of PNM. The shaded green region is the EoS of PNM where the density dependence of symmetry energy is modeled as soft; the red shaded region is the one where the said density dependence is modeled as stiff [56]. The blue shaded region displays the results obtained in the present work; it has an excellent overlap with the "experimental" EoS. Possible phase transitions to exotic phases such as hyperons, kaons, etc. at high densities soften the EoS somewhat; this is not taken into account in the present description.

For completeness, to gauge the applicability of the EoS to higher densities, we calculated the lower limit of the maximum mass of the neutron star (M_{max}^{NS}) with this EoS, solving the general relativistic Tolman-Oppenheimer-Volkoff equation [57]. The EoS for the crust was taken from the Baym, Pethick, and Sutherland model [58]. The EoS for the core region was calculated under the assumption of a charge-neutral uniform plasma of neutrons, protons, electrons, and muons in β equilibrium. The EoS is causal for $0 \leqslant \rho \leqslant 8.3\rho_0$; the central density of the neutron star in our calculation never reaches beyond $\rho \sim 6\rho_0$. Our value of M_{max}^{NS} ($=2.19M_\odot$) is consistent with the currently observed value of $1.97 \pm 0.04 M_\odot$ for

the pulsar PSR J1614-2230 [59] and also the value of $2.01 \pm 0.04 \, M_\odot$ for the pulsar PSR J0348 + 0432 [60]. The presence of exotic degrees of freedom like hyperons in the core of the neutron star is known to pull down the value of $M_{\max}^{\rm NS}$ substantially [61]; however, in the relativistic mean-field (RMF) model, it is also seen that by increasing the strength of coupling of the hyperon to the vector mesons, the effect of hyperons on $M_{\max}^{\rm NS}$ can be much reduced [62]. Recently analyzing different models, Lattimer *et. al* [50,63] constrained the value of the radius $R_{1.4}$ for a neutron star of mass $1.4 M_\odot$ to 12.1 ± 1.1 km with 90% confidence level; our value of $R_{1.4}$ is 11.95 ± 0.75 km. Determination of neutron star radius is, however, not free from uncertainty. Assuming that the neutron star core is best described by a "normal matter" EoS, Guillot et al. [51] find, again in a 90% confidence level, that for astrophysically relevant masses ($M_{\rm NS} \geqslant 0.5 M_\odot$), the neutron star radius is quasiconstant, $R_{\rm NS} = 9.1^{+1.3}_{-1.5}$ km.

IV. CONCLUSIONS

To sum up, from consensus "empirical" inputs for values of some of the key nuclear parameters at saturation and subsaturation densities, we have constructed a Skyrme-type energy density functional for homogeneous nuclear matter. This is then employed to understand the density dependence of the nuclear symmetry energy and incompressibility and to predict values for the important nuclear parameters such as the symmetry slope parameter L_0, the symmetry incompressibility parameter K_τ, and the incompressibility slope parameter $M(\rho)$. Separate estimates of these quantities have been given from different perspectives; sizable uncertainties remain there. The structural edifice for the energy density functional built on a few known input bulk parameters gives coherence to the evaluated values of the observables; their uncertainties can be constrained better provided the input bulk entities are known with better precision. The general agreement of our EoS with the "experimental" one at supranormal densities is interestingly striking. The near concordance of our calculated lower bound of the maximum mass of a neutron star with the experimental observation of a neutron star of mass $M_{\max}^{\rm NS} \sim 2 M_\odot$ is also very noticeable. Inclusion of exotic degrees of freedom in the interior of the star, however, softens the EoS and lowers the value of $M_{\max}^{\rm NS}$, and this needs further investigation.

[1] P. Möller, W. D. Myers, H. Sagawa, and S. Yoshida, Phys. Rev. Lett. **108**, 052501 (2012).

[2] W. D. Myers and W. J. Swiatecki, Ann. Phys. (NY) **55**, 395 (1969).

[3] W. D. Myers and W. J. Swiatecki, Nucl. Phys. A **336**, 267 (1980).

[4] H. Jiang, G. J. Fu, Y. M. Zhao, and A. Arima, Phys. Rev. C **85**, 024301 (2012).

[5] X. Fan, J. Dong, and W. Zuo, Phys. Rev. C **89**, 017305 (2014).

[6] M. Liu, N. Wang, Z.-X. Li, and F.-S. Zhang, Phys. Rev. C **82**, 064306 (2010).

[7] L. Trippa, G. Colò, and E. Vigezzi, Phys. Rev. C **77**, 061304(R) (2008).

[8] A. Carbone, G. Colò, A. Bracco, L.-G. Cao, P. F. Bortignon, F. Camera, and O. Wieland, Phys. Rev. C **81**, 041301(R) (2010).

[9] J. Dong, W. Zuo, J. Gu, and U. Lombardo, Phys. Rev. C **85**, 034308 (2012).

[10] M. Centelles, X. Roca-Maza, X. Viñas, and M. Warda, Phys. Rev. Lett. **102**, 122502 (2009).

[11] M. Warda, X. Viñas, X. Roca-Maza, and M. Centelles, Phys. Rev. C **80**, 024316 (2009).

[12] L.-W. Chen, C. M. Ko, and B.-A. Li, Phys. Rev. C **72**, 064309 (2005).

[13] B.-A. Li, L.-W. Chen, and C. M. Ko, Phys. Rep. **464**, 113 (2008).

[14] M. A. Famiano *et al.*, Phys. Rev. Lett. **97**, 052701 (2006).

[15] D. V. Shetty, S. J. Yennello, and G. A. Souliotis, Phys. Rev. C **75**, 034602 (2007).

[16] B. K. Agrawal, J. N. De, and S. K. Samaddar, Phys. Rev. Lett. **109**, 262501 (2012).

[17] B. K. Agrawal, J. N. De, S. K. Samaddar, G. Colò, and A. Sulaksono, Phys. Rev. C **87**, 051306(R) (2013).

[18] X. Roca-Maza, M. Brenna, G. Colò, M. Centelles, X. Viñas, B. K. Agrawal, N. Paar, D. Vretenar, and J. Piekarewicz, Phys. Rev. C **88**, 024316 (2013).

[19] X. Roca-Maza, M. Brenna, B. K. Agrawal, P. F. Bortignon, G. Colò, L.-G. Cao, N. Paar, and D. Vretenar, Phys. Rev. C **87**, 034301 (2013).

[20] *Topical Issue on Nuclear Symmetry Energy*, edited by B.-A. Li, A. Ramos, G. Verde, and I. Vidana, Special issue of Eur. Phys. J. A 50, 1 (2014).

[21] A. W. Steiner, M. Prakash, J. M. Lattimer, and P. J. Ellis, Phys. Rep. **411**, 325 (2005).

[22] H.-T. Janka, K. Langanke, A. Marek, G. Martínez-Pinedo, and B. Müller, Phys. Rep. **442**, 38 (2007).

[23] L. F. Roberts, G. Shen, V. Cirigliano, J. A. Pons, S. Reddy, and S. E. Woosley, Phys. Rev. Lett. **108**, 061103 (2012).

[24] Z.-G. Xiao, G.-C. Yong, L.-W. Chen, B.-A. Li, M. Zhang, G.-Q. Xiao, and N. Xu, Eur. Phys. J. A **50**, 37 (2014).

[25] B. A. Brown, Phys. Rev. Lett. **111**, 232502 (2013).

[26] E. Khan, J. Margueron, and I. Vidaña, Phys. Rev. Lett. **109**, 092501 (2012).

[27] S. Shlomo, V. M. Kolomietz, and G. Colò, Eur. Phys. J. A **30**, 23 (2006).

[28] B. K. Agrawal, S. Shlomo, and V. K. Au, Phys. Rev. C **72**, 014310 (2005).

[29] M. Dutra, O. Lourenço, J. S. Sá Martins, A. Delfino, J. R. Stone, and P. D. Stevenson, Phys. Rev. C **85**, 035201 (2012).

[30] B. D. Serot and J. D. Walecka, Adv. Nucl. Phys. **16**, 1 (1986).

[31] B. D. Serot and J. D. Walecka, Int. J. Mod. Phys. E **6**, 515 (1997).

[32] M. Brack, C. Guet, and H.-B. Hakansson, Phys. Rep. **123**, 275 (1985).

[33] B. Cochet, K. Bennaceur, J. Meyer, P. Bonche, and T. Duguet, Int. J. Mod. Phy. E **13**, 187 (2004).

[34] L.-W. Chen, B.-J. Cai, C. M. Ko, B.-A. Li, C. Shen, and J. Xu, Phys. Rev. C **80**, 014322 (2009).

[35] C. Constantinou, B. Muccioli, M. Prakash, and J. M. Lattimer, Phys. Rev. C **89**, 065802 (2014).

[36] C.-H. Lee, T. T. S. Kuo, G. Q. Li, and G. E. Brown, Phys. Rev. C **57**, 3488 (1998).

[37] I. Vidaña and I. Bombaci, Phys. Rev. C **66**, 045801 (2002).

[38] G. Colò, U.Garg, and H. Sagawa, Euro. Phys. J A **50**, 26 (2014).

[39] I. Vidaña, C. Providência, A. Polls, and A. Rios, Phys. Rev. C **80**, 045806 (2009).

[40] T. Li *et al.*, Phys. Rev. Lett. **99**, 162503 (2007).

[41] J. Piekarewicz and M. Centelles, Phys. Rev. C **79**, 054311 (2009).

[42] J. Piekarewicz, J. Phys. G **37**, 064038 (2010).

[43] J. M. Pearson, N. Chamel, and S. Goriely, Phys. Rev. C **82**, 037301 (2010).

[44] M. M. Majumdar, S. K. Samaddar, N. Rudra, and J. N. De, Phys. Rev. C **49**, 541 (1994).

[45] G. Arfken and H. Weber, *Mathematical Methods for Physicists* (Academic Press, Waltham, MA, 2005).

[46] C. Ducoin, J. Margueron, C. Providência, and I. Vidaña, Phys. Rev. C **83**, 045810 (2011).

[47] S. Abrahamyan *et al.*, Phys. Rev. Lett. **108**, 112502 (2012).

[48] F. J. Fattoyev and J. Piekarewicz, Phys. Rev. Lett. **111**, 162501 (2013).

[49] C. J. Horowitz and J. Piekarewicz, Phys. Rev. C **64**, 062802(R) (2001).

[50] J. M. Lattimer and A. W. Steiner, Euro. Phys. J **50**, 40 (2014).

[51] S. Guillot, M. Servillat, N. Webb, and R. Rutledge, Astrophys. J **772**, 7 (2013).

[52] C. M. Tarbert, D. P. Watts, D. I. Glazier, P. Aguar *et al.*, Phys. Rev. Lett. **112**, 242502 (2014).

[53] P. Danielewicz, W. G. Lynch, and R. Lacey, Science **298**, 1592 (2002).

[54] C. Fuchs, Prog. Part. Nucl. Phys. **56**, 1 (2006).

[55] A. F. Fantina, N. Chamel, J. M. Pearson, and S. Goriely, EPJ Web Conf. **66**, 07005 (2014).

[56] M. Prakash, T. L. Ainsworth, and J. M. Lattimer, Phys. Rev. Lett. **61**, 2518 (1988).

[57] S. Weinberg, *Gravitation and Cosmology* (Wiley, New York, 1972).

[58] G. Baym, C. Pethick, and P. Sutherland, Astrophys. J. **170**, 299 (1971).

[59] P. B. Demorest, T. Pennucci, S. M. Ransom, M. S. E. Roberts, and J. W. T. Hessels, Nature (London) **467**, 1081 (2010).

[60] J. Antoniadis *et al.*, Science **340**, 448 (2013).

[61] H. J. Schulze and T. Rijken, Phys. Rev. C **84**, 035801 (2011).

[62] S. Weissenborn, D. Chatterjee, and J. Schaffner-Bielich, Phys. Rev. C **85**, 065802 (2012).

[63] J. M. Lattimer and Y. Lim, Astrophys. J. **771**, 51 (2013).